

World Journal of *Diabetes*

World J Diabetes 2022 April 15; 13(4): 282-386



REVIEW

- 282 Insulin-resistance in paediatric age: Its magnitude and implications
Al-Beltagi M, Bediwy AS, Saeed NK

MINIREVIEWS

- 308 Gut microbiota and diabetic kidney diseases: Pathogenesis and therapeutic perspectives
Lin JR, Wang ZT, Sun JJ, Yang YY, Li XX, Wang XR, Shi Y, Zhu YY, Wang RT, Wang MN, Xie FY, Wei P, Liao ZH
- 319 Cognitive disorder and dementia in type 2 diabetes mellitus
Ortiz GG, Huerta M, González-Usigli HA, Torres-Sánchez ED, Delgado-Lara DL, Pacheco-Moisés FP, Mireles-Ramírez MA, Torres-Mendoza BM, Moreno-Cih RI, Velázquez-Brizuela IE

ORIGINAL ARTICLE**Basic Study**

- 338 Roles of transient receptor potential channel 6 in glucose-induced cardiomyocyte injury
Jiang SJ
- 358 Long noncoding RNA X-inactive specific transcript regulates NLR family pyrin domain containing 3/caspase-1-mediated pyroptosis in diabetic nephropathy
Xu J, Wang Q, Song YF, Xu XH, Zhu H, Chen PD, Ren YP

Retrospective Cohort Study

- 376 Risk factors for mortality within 6 mo in patients with diabetes undergoing urgent-start peritoneal dialysis: A multicenter retrospective cohort study
Cheng SY, Yang LM, Sun ZS, Zhang XX, Zhu XY, Meng LF, Guo SZ, Zhuang XH, Luo P, Cui WP

ABOUT COVER

Editorial Board Member of *World Journal of Diabetes*, Da Li, MD, PhD, DSc (Med), Professor, Deputy Director, Center of Reproductive Medicine, Shengjing Hospital of China Medical University, Shenyang 110004, Liaoning Province, China. leeda@ymail.com

AIMS AND SCOPE

The primary aim of *World Journal of Diabetes* (*WJD*, *World J Diabetes*) is to provide scholars and readers from various fields of diabetes with a platform to publish high-quality basic and clinical research articles and communicate their research findings online.

WJD mainly publishes articles reporting research results and findings obtained in the field of diabetes and covering a wide range of topics including risk factors for diabetes, diabetes complications, experimental diabetes mellitus, type 1 diabetes mellitus, type 2 diabetes mellitus, gestational diabetes, diabetic angiopathies, diabetic cardiomyopathies, diabetic coma, diabetic ketoacidosis, diabetic nephropathies, diabetic neuropathies, Donohue syndrome, fetal macrosomia, and prediabetic state.

INDEXING/ABSTRACTING

The *WJD* is now abstracted and indexed in Science Citation Index Expanded (SCIE, also known as SciSearch®), Current Contents/Clinical Medicine, Journal Citation Reports/Science Edition, PubMed, and PubMed Central. The 2021 Edition of Journal Citation Reports® cites the 2020 impact factor (IF) for *WJD* as 3.763; IF without journal self cites: 3.684; 5-year IF: 7.348; Journal Citation Indicator: 0.64; Ranking: 80 among 145 journals in endocrinology and metabolism; and Quartile category: Q3.

RESPONSIBLE EDITORS FOR THIS ISSUE

Production Editor: Rui-Rui Wu; Production Department Director: Xu Guo; Editorial Office Director: Jia-Ping Yan.

NAME OF JOURNAL

World Journal of Diabetes

ISSN

ISSN 1948-9358 (online)

LAUNCH DATE

June 15, 2010

FREQUENCY

Monthly

EDITORS-IN-CHIEF

Lu Cai, Md. Shahidul Islam, Jian-Bo Xiao, Manfredi Rizzo, Michael Horowitz

EDITORIAL BOARD MEMBERS

<https://www.wjgnet.com/1948-9358/editorialboard.htm>

PUBLICATION DATE

April 15, 2022

COPYRIGHT

© 2022 Baishideng Publishing Group Inc

INSTRUCTIONS TO AUTHORS

<https://www.wjgnet.com/bpg/gerinfo/204>

GUIDELINES FOR ETHICS DOCUMENTS

<https://www.wjgnet.com/bpg/GerInfo/287>

GUIDELINES FOR NON-NATIVE SPEAKERS OF ENGLISH

<https://www.wjgnet.com/bpg/gerinfo/240>

PUBLICATION ETHICS

<https://www.wjgnet.com/bpg/GerInfo/288>

PUBLICATION MISCONDUCT

<https://www.wjgnet.com/bpg/gerinfo/208>

ARTICLE PROCESSING CHARGE

<https://www.wjgnet.com/bpg/gerinfo/242>

STEPS FOR SUBMITTING MANUSCRIPTS

<https://www.wjgnet.com/bpg/GerInfo/239>

ONLINE SUBMISSION

<https://www.f6publishing.com>

Basic Study

Long noncoding RNA X-inactive specific transcript regulates NLR family pyrin domain containing 3/caspase-1-mediated pyroptosis in diabetic nephropathy

Jia Xu, Qin Wang, Yi-Fan Song, Xiao-Hui Xu, He Zhu, Pei-Dan Chen, Ye-Ping Ren

Specialty type: Urology and nephrology

Provenance and peer review:

Unsolicited article; Externally peer reviewed.

Peer-review model: Single blind

Peer-review report's scientific quality classification

Grade A (Excellent): A
Grade B (Very good): 0
Grade C (Good): C
Grade D (Fair): 0
Grade E (Poor): 0

P-Reviewer: Ma D, China; Zhang L, China

Received: October 15, 2021

Peer-review started: October 15, 2021

First decision: December 27, 2021

Revised: January 24, 2022

Accepted: March 15, 2022

Article in press: March 15, 2022

Published online: April 15, 2022



Jia Xu, Qin Wang, Yi-Fan Song, Xiao-Hui Xu, He Zhu, Pei-Dan Chen, Ye-Ping Ren, Department of Nephrology, Shenzhen University General Hospital, Shenzhen 518000, Guangdong Province, China

Corresponding author: Ye-Ping Ren, PhD, Chief Doctor, Department of Nephrology, Shenzhen University General Hospital, No. 1098 Xueyuan Road, Nanshan District, Shenzhen 518000, Guangdong Province, China. drrenyeping123@163.com

Abstract

BACKGROUND

NLRP3-mediated pyroptosis is recognized as an essential modulator of renal disease pathology. Long noncoding RNAs (lncRNAs) are active participants of diabetic nephropathy (DN). X inactive specific transcript (XIST) expression has been reported to be elevated in the serum of DN patients.

AIM

To evaluate the mechanism of lncRNA XIST in renal tubular epithelial cell (RTEC) pyroptosis in DN.

METHODS

A DN rat model was established through streptozotocin injection, and XIST was knocked down by tail vein injection of the lentivirus LV sh-XIST. Renal metabolic and biochemical indices were detected, and pathological changes in the renal tissue were assessed. The expression of indicators related to inflammation and pyroptosis was also detected. High glucose (HG) was used to treat HK2 cells, and cell viability and lactate dehydrogenase (LDH) activity were detected after silencing XIST. The subcellular localization and downstream mechanism of XIST were investigated. Finally, a rescue experiment was carried out to verify that XIST regulates NLR family pyrin domain containing 3 (NLRP3)/caspase-1-mediated RTEC pyroptosis through the microRNA-15-5p (miR-15b-5p)/Toll-like receptor 4 (TLR4) axis.

RESULTS

XIST was highly expressed in the DN models. XIST silencing improved renal metabolism and biochemical indices and mitigated renal injury. The expression of inflammation and pyroptosis indicators was significantly increased in DN rats

and HG-treated HK2 cells; cell viability was decreased and LDH activity was increased after HG treatment. Silencing XIST inhibited RTEC pyroptosis by inhibiting NLRP3/caspase-1. Mechanistically, XIST sponged miR-15b-5p to regulate TLR4. Silencing XIST inhibited TLR4 by promoting miR-15b-5p. miR-15b-5p inhibition or TLR4 overexpression averted the inhibitory effect of silencing XIST on HG-induced RTEC pyroptosis.

CONCLUSION

Silencing XIST inhibits TLR4 by upregulating miR-15b-5p and ultimately inhibits renal injury in DN by inhibiting NLRP3/caspase-1-mediated RTEC pyroptosis.

Key Words: Diabetic nephropathy; Pyroptosis; Renal tubular epithelial cell; Long noncoding RNA X-inactive specific transcript; microRNA-15b-5p; Toll-like receptor 4; NLR family pyrin domain containing 3/caspase-1 pathway

©The Author(s) 2022. Published by Baishideng Publishing Group Inc. All rights reserved.

Core Tip: We investigated the mechanism of long noncoding RNA X-inactive specific transcript (XIST) on NLR family pyrin domain containing 3/caspase-1-mediated renal tubular epithelial pyroptosis through the microRNA-15-5p/Toll-like receptor 4 axis and identified XIST as a possible molecular target to mediate renal tubular epithelial pyroptosis in the treatment of renal injury in diabetic nephropathy.

Citation: Xu J, Wang Q, Song YF, Xu XH, Zhu H, Chen PD, Ren YP. Long noncoding RNA X-inactive specific transcript regulates NLR family pyrin domain containing 3/caspase-1-mediated pyroptosis in diabetic nephropathy. *World J Diabetes* 2022; 13(4): 358-375

URL: <https://www.wjgnet.com/1948-9358/full/v13/i4/358.htm>

DOI: <https://dx.doi.org/10.4239/wjd.v13.i4.358>

INTRODUCTION

As a deleterious complication of diabetes and a critical cause of end-stage renal failure, diabetic nephropathy (DN) mainly manifests as morphological and functional abnormalities, such as glomerular hyperfiltration, natriuresis, proteinuria, the dysregulation of cell junction intercellular communication [1] and changes in the structure and function of the kidneys[2]. DN is characterized by thickening of the glomerular basement membranes, glomerular capillary damage, inflammation and oxidative stress, mesangium expansion, and urinary microalbumin[3]. The main process crucial for DN pathogenesis is the increased loss of renal cells, which consequentially leads to renal damage and renal dysfunctions involving alterations in structural integrity and glomerular filtration[4]. DN is triggered by many factors, such as dyslipidaemia, hyperglycaemia, haemodynamic abnormalities, and environmental and genetic causes[5,6]. Additionally, evidence accumulated from experimental and clinical studies indicates that renal inflammation is key to determining the progression of renal injury[7]. Despite the high mortality of diabetic patients with DN, effective treatment remains elusive. Identifying genetic determinants and understanding their roles in DN progression is crucial to develop effective diagnostic tools and treatments.

Pyroptosis, a newly discovered mode of programmed cell death, is characterized by dependence on caspase-1 and NLRP3 inflammasome activation[8]. The participation of pyroptosis in cancers, cardiovascular diseases, and microbial infection-related diseases has been intensively studied[9-11]. Pyroptosis can cause cell death, inflammation, and renal injury, while inhibiting pyroptosis relieves pathological injury[12,13]. The involvement and importance of pyroptosis in DN have recently been clarified[14]. Increasing evidence suggests that pyroptosis and the subsequent inflammatory response play key roles in DN pathogenesis[15-17].

Noncoding RNAs (ncRNAs), such as microRNAs (miRNAs), long noncoding RNAs (lncRNAs), and circular RNAs, participate in DN pathogenesis by regulating inflammation, apoptosis, and other pathological processes[18,19]. A recent study reported that DN progression is closely related to lncRNA expression, which is important for the early diagnosis of DN and targeted interventions[20]. XIST expression is elevated in the serum of DN patients[21]. Silencing XIST protects against renal interstitial fibrosis in DN mice *via* miR-93-5p[22]. XIST also regulates pyroptosis in lung cancer[23], but its effect on renal tubular epithelial cell (RTEC) pyroptosis is unknown. miRNAs are well-known biomarkers used in DN diagnosis, and miRNA profile alterations significantly correlate with DN and renal dysfunction [24]. miR-15b-5p is downregulated in urinary exosomes of DN patients compared with healthy controls [6]. Moreover, the miR-15a-5p-XIST-CUL3 competing endogenous RNA (ceRNA) network is involved in

the mechanism of sepsis-induced acute kidney injury[25]. Whether there is a ceRNA loop involving XIST and miR-15b-5p in RTECs in DN progression is largely unknown. Therefore, we studied the mechanism of lncRNA XIST in RTEC pyroptosis and provide a new theoretical basis for XIST as a molecular target to mediate RTEC pyroptosis in DN management.

MATERIALS AND METHODS

DN model establishment and treatment

Male Sprague-Dawley rats (8 wk, 300-320 g) were provided by Shanghai Experimental Animal Center (Shanghai, China) and raised in a specific pathogen-free animal room at 25 °C under a 12/12 h light-dark cycle with free access to food and water. The model was established after one week of adaptive feeding. Streptozotocin (STZ, 50 mg/kg, S0130, Sigma, United States) was used to establish the DN rat model. STZ was dissolved in 0.1 M citric acid buffer. The DN model was established by injecting STZ (intraperitoneal injection, i.p.) once per day for 5 d. Fasting blood glucose levels were measured 5-7 d after injection, and rats with fasting blood glucose levels above 16.5 mmol/L for 3 consecutive days were identified as successful DN models. Rats in the control group were injected with an equal volume of citrate buffer (P4809, Sigma, United States). The rats were allocated into a control group, DN group, DN + LV-sh-NC group, and DN + LV-sh-XIST group. Each rat was numbered according to its weight and divided into groups according to the random number method. There were 8 rats in each group, for a total of 32 rats. The health status of the rats was monitored every 2 d. If weight loss was > 15%, the rat was euthanized; however, no animals died before the end of the experiment. After successful model establishment (Day 7 after STZ injection), the DN rats were injected with LV-sh-NC or LV-sh-XIST lentiviral interference vectors (200 µL, GenePharma, Shanghai, China). All DN rats were sacrificed by intraperitoneal injection of pentobarbital (100 mg/kg, P-010, Sigma United States) on the 21st day after STZ injection. All appropriate measures were taken to minimize the pain and discomfort of the animals.

Detection of renal metabolic and biochemical indices in rats

The rats were placed in the metabolic cage alone, and urine protein for 24 h (UP 24 h) was collected. On the 20th day after STZ injection, rats in each group fasted overnight and then weighed. Tail vein blood samples were then analyzed by a portable blood glucose meter (OneTouch Ultra Easy, Johnson & Johnson, NJ, United States) to measure fasting blood glucose (FBG). Blood samples were collected from the posterior orbital venous plexus. Serum samples were separated from the blood samples by centrifugation (1000 g, 10 min, 4 °C). The rats were euthanized by excessive pentobarbital (100 mg/kg, i.p.), and the kidney was collected and weighed. KW/BW was calculated according to the following formula:

$$\text{KW/BW} = \text{kidney weight (g)}/\text{body weight (g)}.$$

According to the manufacturer's instructions, blood urea nitrogen (BUN) was detected by a UREA/BUN assay kit (Changchun Huili Biotech, Changchun, China); serum creatinine (Cr) was detected by a Cr assay kit (Huili Biotech); and UP 24 h was detected by an UP assay kit (Nanjing Jiancheng, Nanjing, China). These parameters were analyzed with a 240 or 800 Automated Chemistry Analyser (Rayto, Shenzhen, China).

Histological staining of kidney tissue

The rats were sacrificed, and the kidneys were collected. The kidneys were fixed with 16 g/L paraformaldehyde solution for 24 h and then embedded in paraffin. Serial sections of 4 µm thickness were cut from paraffined blocks and subjected to haematoxylin and eosin (HE), periodic acid Schiff (PAS), and Masson's trichrome staining and observed under a light microscope (TI-S, Nikon, Japan). The pathological analysis was performed by 2 pathologists unaware of this study using ImageJ (NIH, Bethesda, MD, United States). The glomerular volume was calculated as follows: $V = 4/3 \pi (D/2)^3$, where D is the geometric mean of the four diameters. The mesangial matrix index was calculated as follows: mesangial matrix index = mesangial matrix area/global area × 100%. To evaluate tubulointerstitial fibrosis, at least 20 visual fields of each section were analyzed by Masson staining software. Scores from 0 to 3 were used to assess the degree of tubulointerstitial fibrosis: 0, normal interstitium; 0.5, ≤ 5% of area injured; 1, 5%-15% of area injured; 1.5, 16%-25% of area injured; 2, 26%-35% of area injured; 2.5, 36%-45% of area injured; 3, > 45% of area injured[26].

Enzyme-linked immunosorbent assay

Fresh kidney tissue was homogenized in phosphate-buffered saline (PBS) and centrifuged. After total protein quantification, renal tissue samples were used for enzyme-linked immunosorbent assay (ELISA) measurement[27]. At the same time, cell culture supernatant was collected. The expression levels of interleukin-1β (IL-1β, RLB00) and IL-18 (DY521-05) in renal tissue and cells were determined according to the ELISA kit instructions (R&D Systems, Minneapolis, MN, United States).

Western blot analysis

The tissue or cells were lysed with enhanced RIPA lysate (AR0105, Boster, Wuhan, Hubei, China) containing protease inhibitor, and the protein concentration was assessed using a bicinchoninic acid protein quantitative kit (Boster). The protein samples were separated by 10% sodium dodecyl sulfate (SDS)-polyacrylamide gel electrophoresis and transferred to polyvinylidene fluoride membranes. The membranes were then blocked with 5% bovine serum albumin (A1933, Sigma, United States) for 2 h to block nonspecific binding. Next, the membranes were immersed overnight in primary antibody solutions, followed by secondary goat anti-rabbit IgG H&L (HRP) (1:2000, ab205718, Abcam, Cambridge, United Kingdom) or goat anti-mouse IgG (1:2000, ab205719, Abcam, Cambridge, United Kingdom). The proteins were developed using enhanced chemiluminescence (EMD Millipore, Billerica, MA, United States) and analysed using Image-Pro Plus 6.0 (Media Cybernetics, Silver Spring, MD, United States). The primary antibodies were cleaved caspase-1 (1:1000, #89332, CST, Danvers, MA, United States), caspase-1 (1:100, sc-392736, Santa Cruz Biotechnology, Dallas, TX, United States), rabbit monoclonal antibody gasdermin D (GSDMD, 1:1000, ab219800, Abcam, Cambridge, United Kingdom), GSDMD-N (1:1000, PA5-116815, Thermo Fisher, Waltham, MA, United States), NLRP3 (1:1000, ab214185, Abcam, Cambridge, United Kingdom), ASC mouse monoclonal antibody (1:100, sc-514414, Santa Cruz Biotechnology, TX, United States), TLR4 rabbit polyclonal antibody (1:500, ab13867, Abcam, Cambridge, United Kingdom), and GAPDH (1:2500, ab9485, Abcam, Cambridge, United Kingdom).

Immunofluorescence

The kidney was placed on a clean workbench, and the fibrous capsule was stripped using an aseptic technique. Next, 1 cm³ of renal tubular epithelial tissue was removed from the outer skin tissue, washed with normal saline, and fixed with 10% formalin. Sections 4 µm thick were incubated overnight with caspase-1 mouse monoclonal antibody (1:50, sc-392736, Santa Cruz Biotechnology) at 4 °C, and then conjugated with secondary goat anti-mouse IgG (Alexa Fluor® 488) (1:200, ab150113, Abcam, Cambridge, United Kingdom) in the dark for 1 h. After washing in PBS, the slides were incubated with 4',6-diamidino-2-phenylindole (DAPI) (D9542, Sigma, United States) for 3 min, followed by glycerine loading. The fluorescence was evaluated under a fluorescence microscope (Olympus Life Sciences, Tokyo, Japan).

Cell culture and transfection

The human tubular endothelial cell line HK2 from ATCC (Rockville, MD, United States) was cultured in RPMI 1640 medium (Life Technologies, Carlsbad, CA, United States) containing 10% (v/v) foetal bovine serum (FBS, F2442; Sigma, St. Louis, Missouri, United States) at 37 °C with 50 mL/L CO₂. After 24 h of starvation in serum-free medium, HK2 cells were cultured in normal (5 mmol/L, NG) or high (40 mmol/L, HG) glucose (Y0001745, Sigma, United States) for 48 h[28].

The miR-15b-5p mimic and miR-15b-5p inhibitor, siRNA sequence targeting XIST (si-XIST), overexpression TLR4 plasmid (oe-TLR4), and their corresponding controls were provided by GenePharma (Shanghai, China). The cells were transfected using Lipofectamine 2000 (Invitrogen, Carlsbad, CA, United States).

The si-XIST sequences were as follows: si-XIST-1 (SS sequence: GGAAGUACCUACUACUUAAGA, AS Sequence: UUAAGUAGUAGGUACUCCAG), si-XIST-2 (SS sequence: GGUGGACUAUCAACAUAUAAU, AS sequence: UUAUGUUGAUAGUCCACCAG), and si-XIST-3 (SS sequence: GGAAUAGAUAAAUGUCAAG, AS sequence: UUGACAUUUAUCUAAUUCCUU).

Quantitative real-time polymerase chain reaction

Total RNA was extracted using the RNeasy Mini Kit (Qiagen, Valencia, CA, United States). A reverse transcription kit (RR047A, Takara, Tokyo, Japan) was used to obtain cDNA. A miRNA first-strand cDNA synthesis kit (B532451-0020, Sangon, Shanghai, China) was used for miRNA detection.

SYBR Premix Ex Taq II (DRR081, Takara) and real-time fluorescence qPCR (7500, ABI, Foster City, CA, United States) were used for the qRT-PCR experiment. The PCR primers (Table 1) were designed and synthesized by Sangon. GAPDH or U6 was the internal reference. Gene expression was calculated using the 2^{-ΔΔt} method.

Cell viability measurement

The viability of HK2 cells was detected by a Cell Titer Glo Luminescent Cell Viability Assay Kit (G7570, Promega, Beijing, China). Cells (10⁵) were seeded into 6-well plates containing normal growth medium and then collected when the confluence reached 80%-90%. Before collecting the HK2 cells, the reagents were prepared, and then the cells (50 µL) were loaded into black-walled 96-well plates that contained the same amount of final substrate solution. After mixing for 10 min, the cells were incubated in a plate-reading luminometer (Varioskan™, Thermo Scientific, Rockford, IL, United States).

Lactate dehydrogenase (LDH) release assay

An LDH release assay kit (Beijing, Nanjing, China) was used to detect cytotoxicity. HG-treated HK2 cells were plated into 96-well plates and incubated at 37 °C with 50 mL/L CO₂ for 24 h. The cell medium was

Table 1 Primer sequences

	Forward Primer (5'-3')	Reverse Primer (5'-3')
XIST (human)	AGCTCCTCGGACAGCTCTAA	CTCCAGATAGCTGGCAACC
XIST (Norway rat)	CCCATACCCCTACATCCCTAATG	GGCTGGCCTCATTTCGGGCTC
hsa-miR-15b-5p	ATCCAGTGGTGTCTGIG	TGCTTAGCAGCACATCATG
rno-miR-15b-5p	GCCGAGTAGCAGCACATCATG	CTCAACTGGTGTCTGTTGA
hsa-pre-miR-15b	GGCCTTAAAGTACTGTAGCAGC	CTCAACTGGTGTCTGTTGA
rno-pre-miR-15b	GGAGTTTTTCCCITTTGGATG	ATAATGATTTCGCATCTTGATGTAG
TLR4 (human)	CCGCTCTGGCATCATCTTCA	TGGGTTTTAGGCGCAGAGTT
TLR4 (Norway rat)	GCCAGGATGATGCCTCTCTTGC	CCTCAGGTCAAAGTTGTTC
U6 (human)	GCTCGCTTCGGCAGCACA	GAGGTATTCCGACCAGAGGA
U6 (Norway rat)	ATGGCGGACGACGTAGATCAGCA	TCAGCCAACCTCTCAATGGAGGGG
GAPDH (human)	TCCATGACAACCTTTGGCATC	CATGTCAGATCCACCACGGA
GAPDH (Norway rat)	CAAGATGGTGAAGGTCGGTGT	CTTACTCCTTGGAGGCCATGTAG

XIST: X inactive specific transcript; TLR4: toll like receptor 4; hsa: *Homo sapiens*; rno: *Rattus norvegicus*; U6: U6 small nuclear RNA; GAPDH: glyceraldehyde-3-phosphate dehydrogenase; pre: precursor; miR: microRNA.

then collected, and LDH activity was measured.

Fluorescence in situ hybridization

Fluorescence in situ hybridization (FISH) was used to identify the subcellular localization of XIST in HK2 cells. In accordance with the instructions of the Ribo™ lncRNA FISH probe mix (Red) (RiboBio, Guangzhou, Guangdong, China), the cover glass was placed into the 6-well culture plate, and HK2 cells were seeded onto it. The confluence was approximately 80% after 1 d of culture. The slides were then washed with PBS and fixed with 1 mL of 16 g/L paraformaldehyde. The slides were treated with proteinase K (2 µg/mL), glycine, and ethylphthalein reagent and then incubated with 250 µL of prehybridizing solution at 42 °C for 1 h. Next, the prehybridizing solution was removed, and 250 µL of hybridizing solution containing probe (300 ng/mL) was added to the slides for hybridization at 42 °C overnight. Following 3 washes with PBS containing 0.05% (v/v) Tween-20 (PBST), DAPI (1:800) diluted with PBST was added to stain the nuclei; the slides were then transferred to 24-well culture plates and incubated for 5 min. The slides were then sealed using an anti-fluorescence quenching agent and photographed using a fluorescence microscope (Olympus)[29].

Nuclear/cytosol fractionation

HK2 cells were resuspended in hypotonic buffer A [10 mm HEPES (pH 7.5), 0.5 mm DTT, 10 mmol/L KCl, 1.5 mmol/L MgCl₂] containing protease inhibitor and RNase inhibitor (N8080119, Thermo Fisher Scientific). The HK2 cells were then incubated on ice for 10 min and centrifuged (1000 × g, 4 °C, 10 min). The supernatant was further centrifuged at 15000 × g for 15 min to obtain the cytoplasmic component. The precipitate was washed twice with hypertonic buffer, resuspended in hypotonic buffer B [10 mm HEPES (pH 7.5), 10 mmol/L KCl, 1.5 mmol/L MgCl₂, 0.5 mm DTT, 0.5% Nonidet P-40], incubated at 4 °C for 30 min, and then centrifuged at 6000 × g, 4 °C and for 10 min. The precipitate was rinsed once with hypertonic buffer and resuspended in RIPA buffer containing protease inhibitor and RNase inhibitor [50 mm Tris HCl (pH 7.5), 1500 mmol/L KCl, 1% Nonidet P-40, 0.5% sodium hydroxide, 0.1% SDS, 1 mmol/L EDTA, pH 8.0], incubated at 4 °C for 30 min, rotated gently, and then centrifuged at 15000 × g for 20 min. The supernatant contained the nuclei[30].

Dual-luciferase assay

The binding sites of XIST and miR-15b-5p, miR-15b-5p and TLR4 were predicted by the bioinformatics website StarBase (<http://starbase.sysu.edu.cn/index.php>). The binding site sequences or their mutants were amplified and inserted into the pmiR vector (Huayueyang, Beijing, China) to construct the wild-type (WT) or mutant (MUT) vectors XIST-WT, TLR4-WT, XIST-MUT, and TLR4-MUT. Subsequently, HEK293T cells (Beinuo, Shanghai, China) were cotransfected with mimic NC or miR-15b-5p mimic for 48 h, after which the cells were collected and lysed, and the luciferase activity was detected using a kit (K801-200; Biovision, Mountain View, CA, United States).

RNA immunoprecipitation

The binding of miR-15b-5p to TLR43 and XIST was detected by an RNA immunoprecipitation (RIP) kit (Millipore, MA, United States). HK2 cells were rinsed with precooled PBS, and the supernatant was discarded. The cells were incubated with an equal volume of RIPA lysate (P0013B, Beyotime, Shanghai, China) for 5 min and centrifuged at 4 °C for 10 min to obtain the supernatant. One part of the cell extract was taken as input, and the other part was incubated with the antibody for coprecipitation. RNA was extracted from the sample after detachment with proteinase K and used for qRT-PCR of XIST, miR-15b-5p, and TLR4. The antibodies used in RIP were AGO2 (1:100, ab32381, Abcam, Cambridge, United Kingdom) and rabbit anti-IgG (1:100, ab109489, Abcam, Cambridge, United Kingdom), which was used as the control.

Statistical analysis

The statistical review of the study was performed by a biomedical statistician. SPSS 21.0 (IBM Corp. Armonk, NY, United States) was used to process the data, and GraphPad Prism 8.0 (GraphPad Software, San Diego, CA, United States) was used for mapping. All measurement data were tested for normal distribution and homogeneity of variance and are presented as the mean \pm SD. The comparisons among multiple groups were conducted by one-way or two-way analysis of variance (ANOVA), followed by Tukey's multiple comparisons test. A probability value of $P < 0.05$ implied a statistically significant difference.

RESULTS

Silencing lncRNA XIST inhibits STZ-induced renal injury in DN rats

An increasing number of studies have focused on the regulatory mechanism of lncRNAs in DN development. XIST is upregulated in acute kidney injury, and inhibiting XIST can alleviate acute kidney injury[31]. However, the regulatory mechanism of XIST in DN requires further exploration.

To study the role of XIST in DN, we first established a DN rat model and detected XIST expression. XIST in the DN group was higher than that in the control group. We then used LV-sh-XIST lentivirus to knock down XIST expression in the model rats ($P < 0.05$, Figure 1A) and detected the renal metabolic and biochemical indices (including KW/BW, FBG, BUN, Cr, and UP 24 h) of the rats. The KW/BW, FBG, BUN, Cr, and UP 24 h values in DN rats were higher than those in control rats, while LV-sh-XIST injected *via* the caudal vein significantly reduced these indices (except for FBG) (all $P < 0.05$, Figure 1B-F). Meanwhile, we detected the histological changes in renal tissue by HE staining, PAS staining, and Masson staining. Compared with the control group, the DN and DN + LV-sh-NC groups had several abnormalities, such as glomerular hypertrophy, basement membrane thickening, mesangial hyperplasia, glomerular epithelial cell swelling, lumen stenosis, inflammatory cell infiltration, and moderate fibrosis. Lentivirus LV-sh-XIST intervention improved all of these histological changes ($P < 0.05$, Figure 1G). Thus, silencing XIST can inhibit renal injury in DN rats.

Silencing XIST inhibits pyroptosis in DN rats

Inflammation is an important pathogenic factor of DN that can lead to RTEC pyroptosis[28]. However, no studies have investigated the effects of XIST on pyroptosis in DN. Here, we detected IL-1 β and IL-18 expression in renal tissue. ELISA revealed that IL-1 β and IL-18 in the DN group were elevated, but they were lowered after silencing XIST ($P < 0.05$, Figure 2A). Western blot analysis showed that the NLRP3, ASC, cleaved caspase-1, caspase-1, GSDMD, and GSDMD-N levels in the DN group were significantly enhanced, but they were lowered after silencing XIST (all $P < 0.05$, Figure 2B). The caspase-1 immunofluorescence results were consistent with the Western blot results ($P < 0.05$, Figure 2C). These results suggest that silencing XIST in DN can prevent RTEC pyroptosis.

Silencing XIST inhibits pyroptosis in HG-induced HK2 cells

HK2 cells were treated with HG to further study the regulatory effect of XIST on RTEC pyroptosis *in vitro*. qRT-PCR found that HG treatment induced high XIST expression, while XIST was significantly decreased after transfection of a siRNA sequence targeting XIST ($P < 0.05$, Figure 3A). Si-XIST-1, which had the best silencing efficiency, was used in subsequent experiments. Next, we examined the effect of silencing XIST on RTEC pyroptosis after HG treatment. HG treatment significantly promoted the expression of IL-1 β and IL-18 (as detected by ELISA), as well as NLRP3, ASC, cleaved caspase-1, caspase-1, GSDMD, and GSDMD-N (as shown by Western blot), while these levels were significantly lower after silencing XIST (all $P < 0.05$, Figure 3B-C). Silencing XIST also annulled the inhibition of HK2 cell viability by HG ($P < 0.05$, Figure 3D) and significantly reduced the release rate of LDH ($P < 0.05$, Figure 3E). Overall, silencing XIST inhibited HG-induced RTEC pyroptosis *in vitro*.

lncRNA XIST binds to miR-15b-5p in DN

To further study the regulatory mechanism of XIST on RTEC pyroptosis in DN, we first used FISH and

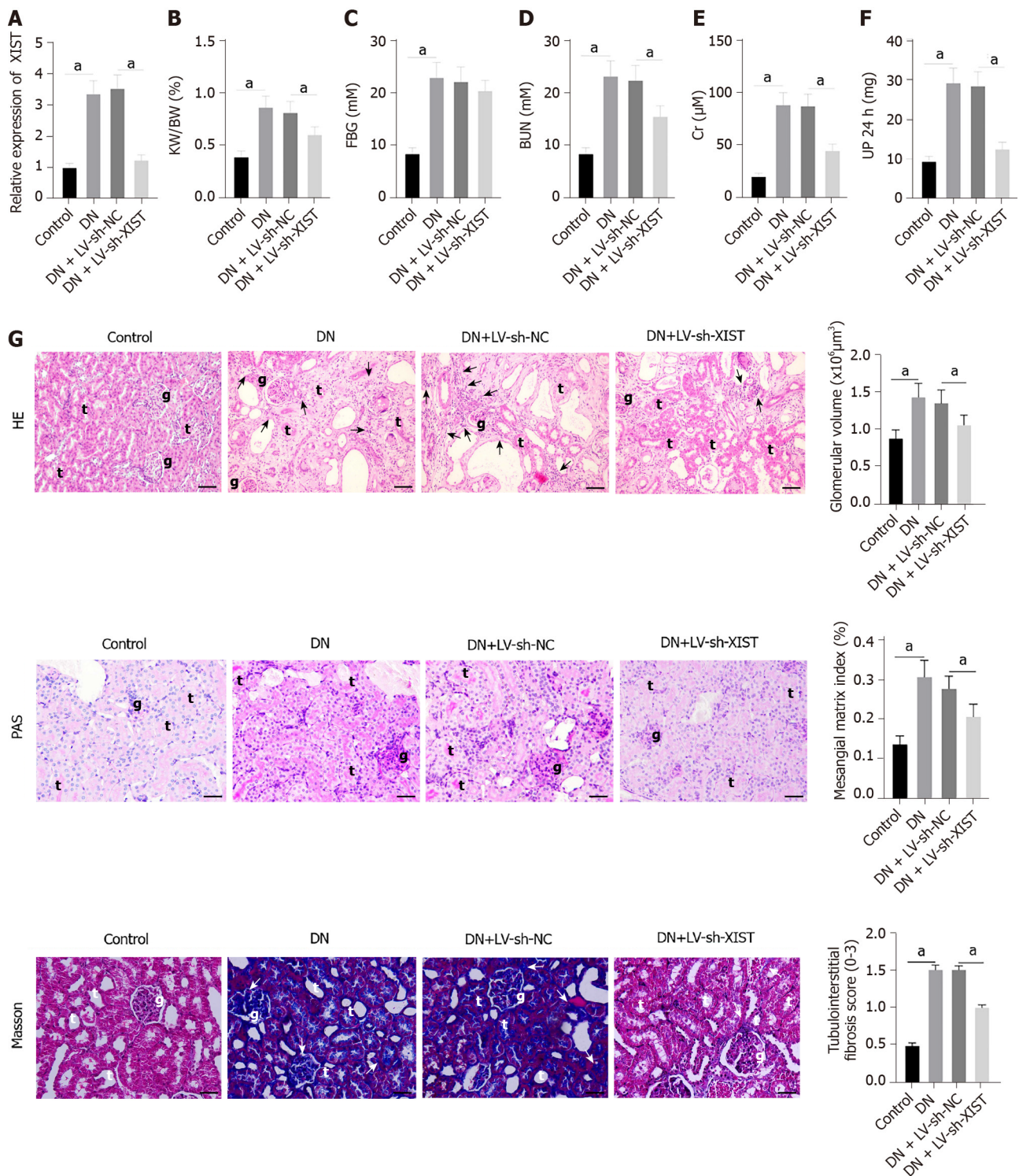


Figure 1 Silencing lncRNA X inactive specific transcript can inhibit renal injury in DN rats. After establishing DN model rats, lentivirus-LV sh-X inactive specific transcript (XIST) was injected into the tail vein to knock down XIST expression *in vivo*. A: XIST expression detected by qRT-PCR; B: Kidney weight/body weight (KW/BW); C: Fasting blood glucose (FBG); D: Blood urea nitrogen (BUN); E: Serum creatinine (Cr); F: Urine protein for 24 h (UP 24 h); G: Histological changes of renal tissue estimated by HE staining, PAS staining and Masson staining; scale bar: 25 μm; arrows indicate inflammatory cell infiltration (black arrows) and fibrosis (white arrows). (g) glomerulus, (t) tubules; n = 8/group. The data were described as mean ± SD and analyzed by one-way ANOVA and Tukey's multiple comparisons test; ^aP < 0.05. DN: Diabetic nephropathy; LV: Lentivirus; XIST: X inactive specific transcript; sh: Short hairpin RNA; HE: Hematoxylin-eosin staining; PAS: Periodic Acid-Schiff stain.

nuclear/cytosolic fractionation to identify that XIST was mainly expressed in the cytoplasm (Figure 4A-B). These results indicated that XIST may play a role in DN *via* a ceRNA loop. StarBase (<http://starbase.sysu.edu.cn/index.php>) predicted that XIST can bind to miR-15b-5p (Figure 4C). The dual-luciferase experiment ($P < 0.05$, Figure 4D) and RIP experiment verified that XIST could adsorb and bind to miR-15b-5p ($P < 0.05$, Figure 4E). qRT-PCR showed that miR-15b-5p in the DN group was

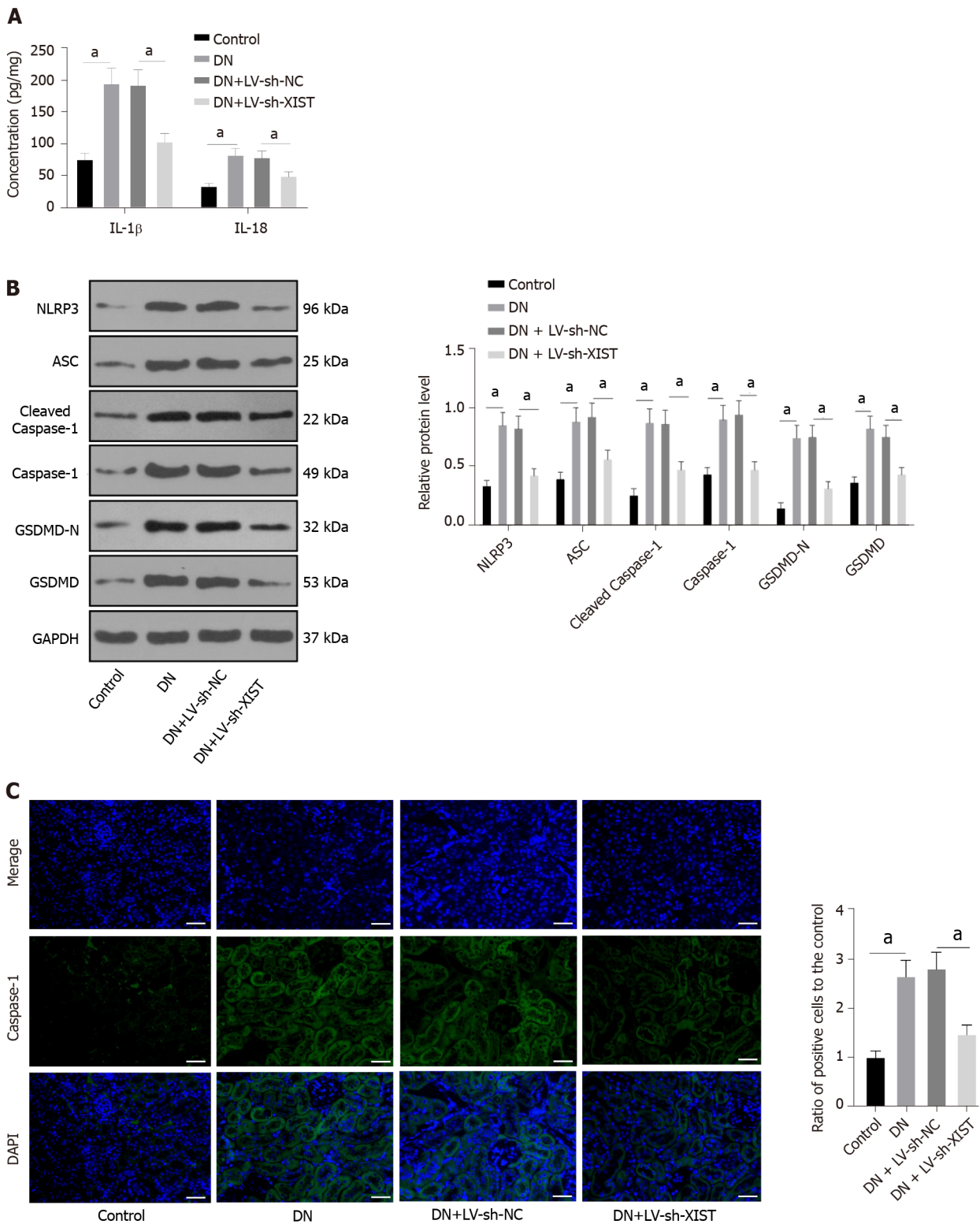


Figure 2 Silencing lncRNA X inactive specific transcript can inhibit renal tubular epithelial cell pyroptosis in diabetic nephropathy rats. After establishing diabetic nephropathy model rats, lentivirus-LV sh- X inactive specific transcript was injected into the tail vein. A: Enzyme-linked immunosorbent assay detected IL-1 β and IL-18 expressions; B: Western blot tested the levels of NLR family pyrin domain containing 3, ASC, Cleaved Caspase-1, Caspase-1, GSDMD, and GSDMD-N; C: Immunofluorescence tested the expression of Caspase-1; scale bar: 25 μ m; N = 8/group. The data were described as mean \pm SD and analyzed by one-way ANOVA and Tukey's multiple comparisons test; * $P < 0.05$. DN: Diabetic nephropathy; LV: Lentivirus; XIST: X inactive specific transcript; sh: Short hairpin RNA; NLRP3: NLR family pyrin domain containing 3; ASC: Apoptosis speck-like protein; GSDMD: Gasdermin D; DAPI: 4',6-diamidino-2-phenylindole.

significantly lower and was increased after silencing XIST ($P < 0.05$, Figure 4F). Moreover, miR-15b-5p in HK2 cells was inhibited by HG treatment and was significantly enhanced after silencing XIST ($P < 0.05$, Figure 4G). There was no significant difference in the expression of premiR-15b in rats and cells in each group. These results show that XIST can adsorb and bind to miR-15b-5p to reduce miR-15b-5p

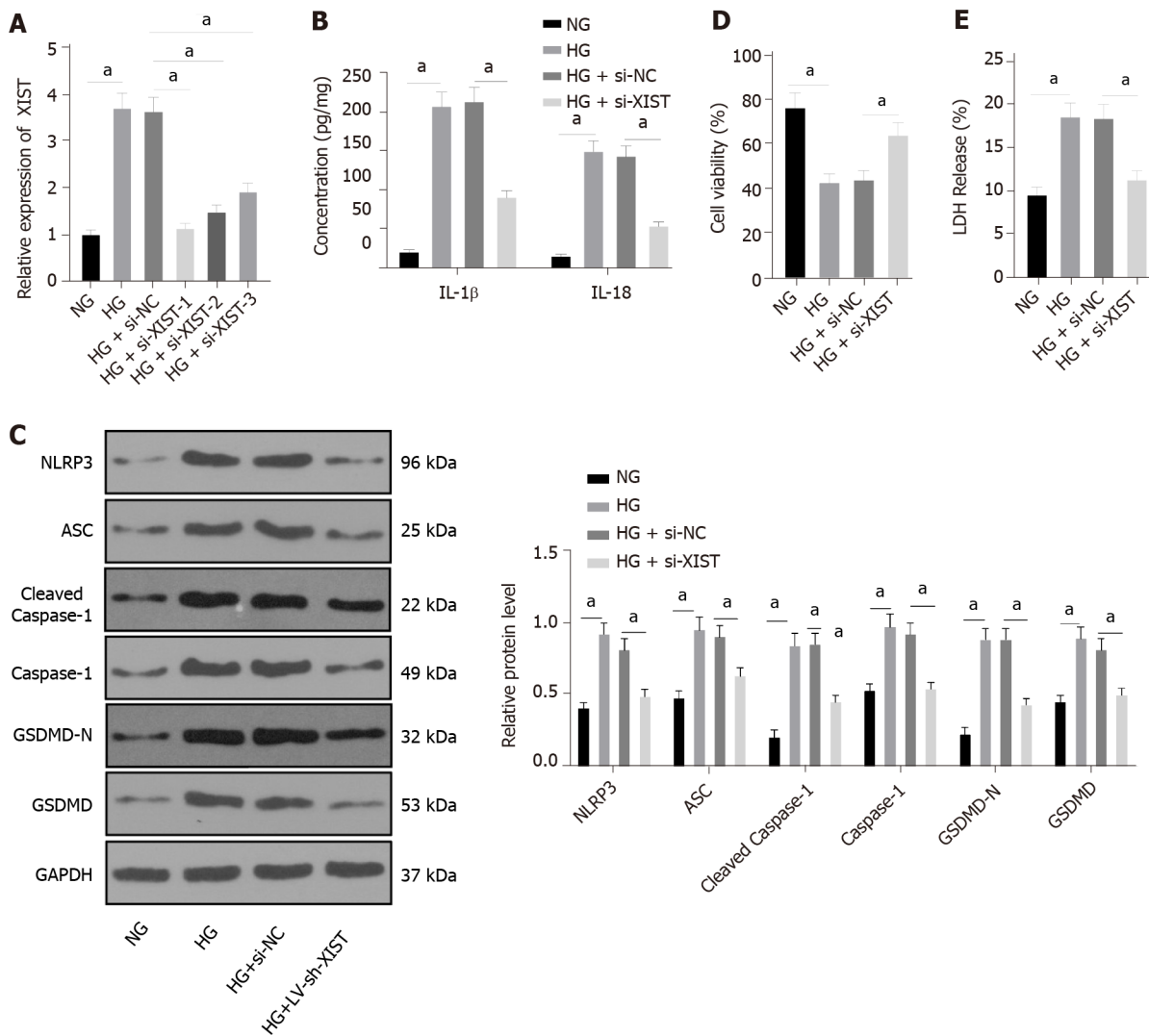


Figure 3 Silencing X inactive specific transcript in diabetic nephropathy can inhibit renal tubular epithelial cell pyroptosis in high glucose-induced HK2 cells. si-NC or si-X inactive specific transcript (XIST) was delivered into HK2 cells treated with high glucose. A: The XIST expression detected by qRT-PCR; B: Enzyme-linked immunosorbent assay detected the expression of IL-1β and IL-18; C: Western blot tested the levels of NLR family pyrin domain containing 3, ASC, Cleaved Caspase-1, Caspase-1, GSDMD, and GSDMD-N; D: Cell viability; E: Lactate dehydrogenase activity. The cell experiment was performed in triplicate. The data were described as mean ± SD and analyzed by one-way ANOVA (A/D-E) or two-way ANOVA (B/C) and Tukey's multiple comparisons test; **P* < 0.05. NG: Normal glucose; HG: High glucose; si: Small interfering RNA; XIST: X inactive specific transcript; LDH: Lactate dehydrogenase; NLRP3: NLR family pyrin domain containing 3; SC: Apoptosis speck-like protein; GSDMD: Gasdermin D.

expression in DN.

Inhibition of miR-15b-5p in XIST-silenced HK2 cells activates RTEC pyroptosis

Next, we carried out functional rescue experiments to verify the above regulatory mechanism. We silenced both XIST and miR-15b-5p in HG-exposed HK2 cells. First, we detected miR-15b-5p expression by qRT-PCR, which verified the transfection efficiency of the miR-15b-5p inhibitor (*P* < 0.05, Figure 5A). In HG-treated HK2 cells, the miR-15b-5p inhibitor reversed the inhibitory effect of si-XIST on IL-1β and IL-18 (all *P* < 0.05, Figure 5B); it also reversed the expression of NLRP3, ASC, cleaved caspase-1, caspase-1, GSDMD, and GSDMD-N (all *P* < 0.05, Figure 5C). Compared with the si-XIST + inhibitor NC group, the cell viability of the si-XIST + miR-15b-5p inhibitor group was decreased (*P* < 0.05, Figure 5D), while the release rate of LDH was increased (*P* < 0.05, Figure 5E). Taken together, these results indicate that silencing XIST inhibits HG-induced RTEC pyroptosis *in vitro* by promoting miR-15b-5p.

LncRNA XIST sponges miR-15b-5p to inhibit TLR4

To study the downstream mechanism of miR-15b-5p, we utilized the StarBase website (<http://starbase.sysu.edu.cn/index.php>) to predict that miR-15b-5p can bind to the 3'UTR of TLR4 (Figure 6A). The dual-luciferase assay and RIP assay also showed that TLR4 was the direct target gene of miR-15b-5p (*P* < 0.05, Figure 6B-C). TLR4 expression in renal tissue was assessed by qRT-PCR and Western blot. The results showed that TLR4 in renal tissue of the DN group was higher than that of the control group, and

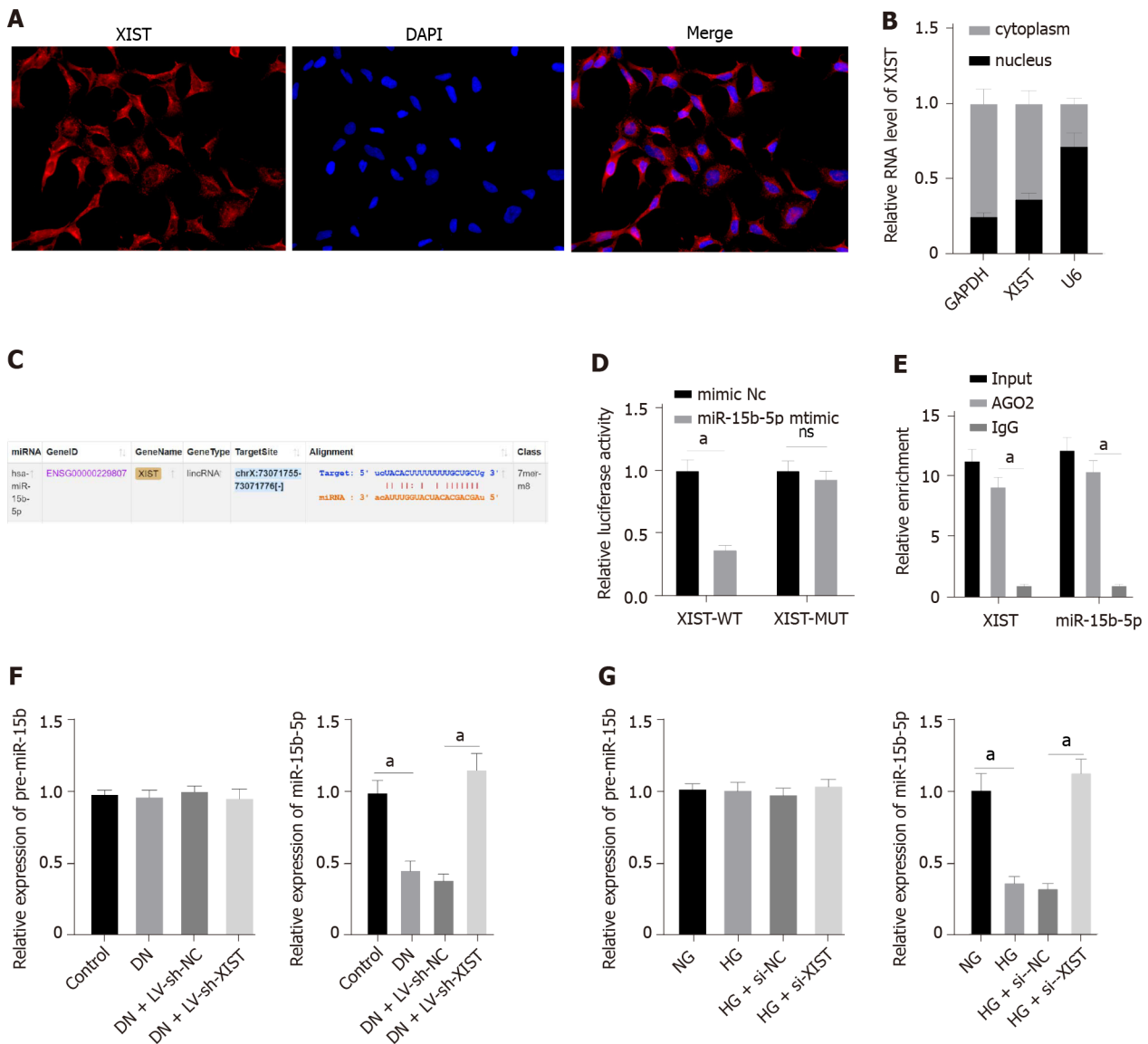


Figure 4 X inactive specific transcript can adsorb and bind to miR-15b-5p to reduce miR-15b-5p expression in diabetic nephropathy. A: Fluorescence in situ hybridization assay (scale bar: 25 μ m); B: Nuclear/cytoplasmic fractionation assay verified the subcellular localization of X inactive specific transcript (XIST) in HK2 cells; C: Starbase website (starbase.sysu.edu.cn/index.php) predicted the binding sites of XIST and miR-15b-5p; D: Dual-luciferase experiment and E: RNA immunoprecipitation experiment verified the binding relation of XIST and miR-15b-5p; F: qRT-PCR detected miR-15b-5p and pre-miR-15b expression in renal tissue; G: qRT-PCR detected miR-15b-5p and pre-miR-15b expression in HK2 cells. The cell experiment was performed in triplicate. The data were described as mean \pm SD and analyzed by one-way ANOVA (F/G) or two-way ANOVA (D/E) and Tukey's multiple comparisons test; $^aP < 0.05$. XIST: X inactive specific transcript; DN: Diabetic nephropathy; DAPI: 4',6'-diamidino-2-phenylindole; GAPDH: Glyceraldehyde-3-phosphate dehydrogenase; U6: U6 small nuclear RNA; WT: Wild type; MUT: Mutant.

TLR4 was lower after silencing XIST (all $P < 0.05$, Figure 6D-E). Additionally, silencing XIST significantly reversed the TLR4 expression induced by HG, while the miR-15b-5p inhibitor reversed the inhibitory effect of silencing XIST (all $P < 0.05$, Figure 6F-G). In summary, XIST inhibits TLR4 expression by binding to miR-15b-5p.

TLR4 overexpression in XIST-silenced cells causes increased pyroptosis

TLR4 promotes apoptosis by activating NLRP3/caspase-1 in hepatic ischaemia-reperfusion injury[32]. Whether XIST regulates HG-induced RTEC pyroptosis through TLR4 remains to be explored.

To further verify the regulatory effect of XIST on TLR4, we silenced XIST and overexpressed TLR4 in HG-treated HK2 cells and detected the TLR4 Levels. TLR4 was significantly overexpressed ($P < 0.05$, Figure 7A-B). Compared with the si-XIST + oe-NC group, TLR4 overexpression promoted IL-1 β and IL-18 expression and increased the levels of NLRP3, ASC, cleaved caspase-1, caspase-1, GSDMD, and GSDMD-N (all $P < 0.05$, Figure 7C-D). Furthermore, TLR4 overexpression decreased cell viability ($P < 0.05$, Figure 7E) and increased the release rate of LDH ($P < 0.05$, Figure 7F). In summary, silencing XIST inhibits HG-induced RTEC pyroptosis by inhibiting TLR4.

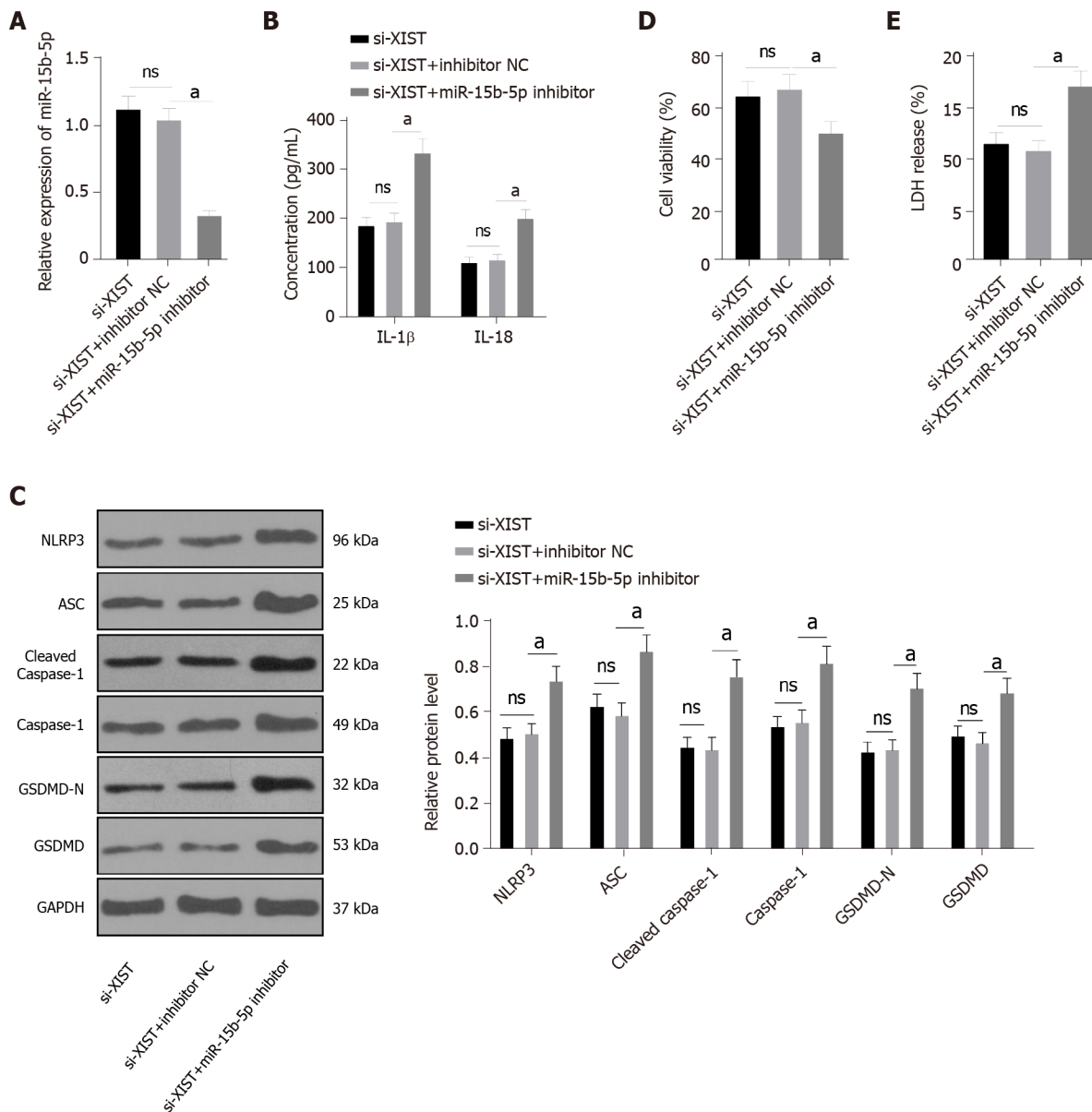


Figure 5 Inhibition of miR-15b-5p in X inactive specific transcript-silenced HK2 cells activates renal tubular epithelial cell pyroptosis. In HG-treated HK2 cells, both X inactive specific transcript (XIST) and miR-15b-5p were silenced. A: qRT-PCR verified the transfection efficiency of miR-15b-5p inhibitor; B: Enzyme-linked immunosorbent assay detected the expression of IL-1 β and IL-18; C: Western blot tested the levels of NLR family pyrin domain containing 3, ASC, Cleaved Caspase-1, Caspase-1, GSDMD, and GSDMD-N; D: Cell viability; E: Lactate dehydrogenase activity. The cell experiment was performed in triplicate. The data were described as mean \pm SD and analyzed by one-way ANOVA (A/D-E) or two-way ANOVA (B/C) and Tukey's multiple comparisons test; ^a*P* < 0.05. LDH: Lactate dehydrogenase; XIST: X inactive specific transcript; si: Small interfering RNA; NLRP3: NLR family pyrin domain containing 3; ASC: Apoptosis speck-like protein; GSDMD: Gasdermin D.

DISCUSSION

As the most prevalent, disastrous, and costly complication of diabetes, DN occurs in approximately 30% to 40% of diabetic patients, representing a considerable public health problem[33]. Pyroptosis and the subsequent inflammatory response are dominant events in DN pathogenesis[15]. This study found that DN induces RTEC pyroptosis by activating NLRP3/caspase-1 and inducing high XIST expression. Silencing XIST promoted the targeted inhibition of TLR4 by miR-15b-5p by upregulating miR-15b-5p, thus inhibiting TLR4 and finally alleviating renal injury in DN rats by inhibiting NLRP3/caspase-1-mediated RTEC pyroptosis (Figure 8).

XIST silencing has been shown to alleviate certain biological processes and inflammation in HG-treated human mesangial cells (HMCs)[21]. XIST was found to be highly expressed in renal tissue of DN patients, STZ-treated DN mice, and HG-exposed HK-2 cells[22]. Consistently, the STZ (50 mg/kg)-induced DN rat model in our study showed the upregulation of XIST. XIST expression was downregulated by LV-sh-XIST lentivirus, and renal metabolic and biochemical indices were detected. The results showed that LV-sh-XIST significantly reduced the values of KW/BW, BUN, Cr, and UP 24 h. FBG is a

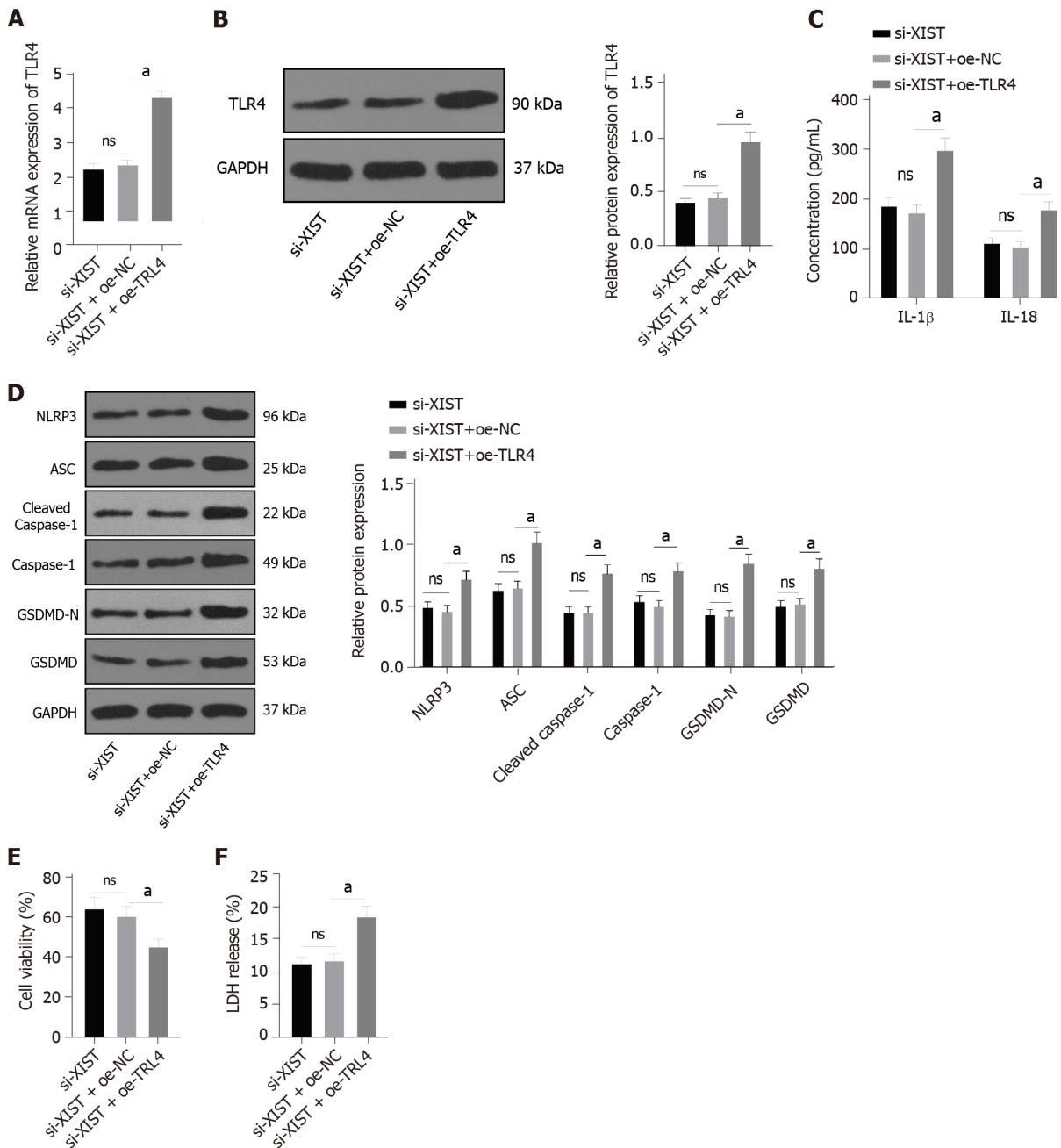


Figure 7 Toll like receptor 4 overexpression in X inactive specific transcript-silenced cells causes increased pyroptosis. In HG-treated HK2 cells, X inactive specific transcript (XIST) was silenced and toll like receptor 4 (TLR4) was overexpressed. A and B: The expression of TLR4 levels detected by qRT-PCR and Western blot; C: Enzyme-linked immunosorbent assay detected the expression of IL-1β and IL-18; D: Western blot tested the levels of NLR family pyrin domain containing 3, ASC, Cleaved Caspase-1, Caspase-1, GSDMD, and GSDMD-N; E: Cell viability; F: LDH activity. The cell experiment was performed in triplicate. The data were described as mean ± SD and analyzed by one-way ANOVA (A/B/E/F) or two-way ANOVA (C/D) and Tukey's multiple comparisons test; ^a*P* < 0.05. XIST: X inactive specific transcript; GAPDH: Glyceraldehyde-3-phosphate dehydrogenase; LDH: Lactate dehydrogenase; NLRP3: NLR family pyrin domain containing 3; ASC: Apoptosis speck-like protein; GSDMD: Gasdermin D.

basement membrane thickening, mesangial hyperplasia, glomerular epithelial cell swelling, lumen stenosis, inflammatory cell infiltration, and fibrosis; however, LV-sh-XIST intervention improved these histological changes. Preventing glomerular hypertrophy and attenuating glomerular hyperfiltration may have therapeutic potential for DN[35]. Consistently, prior work suggests that XIST knockdown alleviates acute kidney injury[31]. These results suggest that silencing lncRNA XIST can inhibit renal injury in DN rats.

Inflammation and RTEC pyroptosis are hallmarks of tubular cell damage and renal functional deterioration in kidney injury[36]. The urinary level of the inflammatory mediator IL-18 has been reported to be positively linked with DN progression[37]. The participation of pyroptosis in DN progression has recently attracted much attention[38,28], and we investigated inflammation and RTEC pyroptosis-related factors. Our results revealed that the IL-1β and IL-18 levels in DN rats were elevated, but they

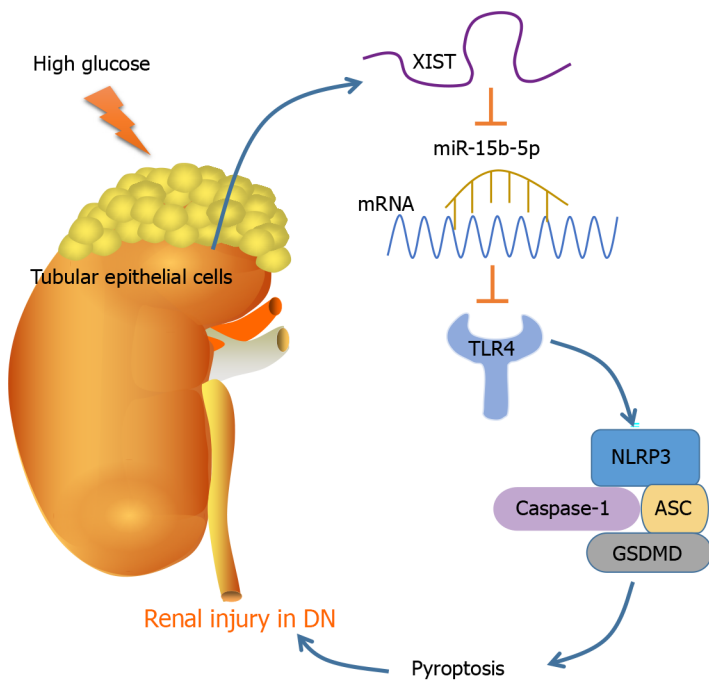


Figure 8 Mechanism diagram. STZ and HG treatment induced high expression of X inactive specific transcript (XIST); silencing XIST promoted the targeted inhibition of miR-15b-5p on toll like receptor 4 (TLR4) by upregulating miR-15b-5p, thereby inhibiting TLR4, and ultimately alleviating the renal injury of diabetic nephropathy by inhibiting NLRP3/Caspase-1-mediated RTEC pyroptosis. mRNA: messenger RNA; DN: Diabetic nephropathy; NLRP3: NLR family pyrin domain containing 3; ASC: Apoptosis speck-like protein; GSDMD: Gasdermin D.

were lower after silencing XIST. Western blot and caspase-1 immunofluorescence showed that the NLRP3, ASC, caspase-1, and GSDMD levels in the DN group were enhanced, but they were lower after silencing XIST, which was highly consistent with previous studies[39,34]. NLRP3 inflammasome activation is related to cell pyroptosis[40]; therefore, the inhibition of NLRP3 inflammatory bodies may be a potential option for DN treatment[41]. To further study the regulatory effect of XIST on pyroptosis, HK2 cells were treated with HG to further study the regulatory effect of XIST on RTEC pyroptosis *in vitro*. Our results revealed that silencing XIST inhibited HG-induced RTEC pyroptosis *in vitro*, reversed the inhibitory effect of HG on HK2 cell viability, and reduced the release rate of LDH. Podocytes exposed to 30 mM HG showed significantly elevated levels of caspase-11, GSDMD-N, IL-1 β , and IL-18, indicating that pyroptosis is activated under hyperglycaemic conditions and during DN development [14]. Collectively, the results indicate that silencing XIST in DN can inhibit HG-induced RTEC pyroptosis.

To further study the regulatory mechanism of XIST on RTEC pyroptosis in DN, we used FISH and nuclear/cytosolic fractionation to identify that XIST was mainly expressed in the cytoplasm. These results suggest that XIST plays a role in DN by regulating ceRNAs. StarBase predicted that XIST can bind to miR-15b-5p, which was validated by dual-luciferase experiments and RIP. qRT-PCR showed that miR-15b-5p in the DN models was significantly lower but increased after silencing XIST. Accordingly, miR-15b-5p was found to be downregulated in the serum of DN patients and in HG-treated HMCs[42]. XIST can adsorb and bind to miR-15b-5p to reduce miR-15b-5p expression in DN. We did not investigate whether XIST undergoes nuclear translocation in the DN models or in HG-treated HK-2 cells. We will focus on this question in future research to provide a more comprehensive mechanism for the role of XIST in DN.

We next carried out functional rescue experiments to verify the postulated regulatory mechanism. XIST and miR-15b-5p were both silenced in HG-treated HK2 cells. Accordingly, the miR-15b-5p inhibitor significantly reversed the inhibitory effect of si-XIST on IL-1 β , IL-18, NLRP3, ASC, caspase-1, and GSDMD; the cell viability was decreased, while the release rate of LDH was significantly increased. Similarly, a previous study revealed that forced expression of miR-15b-5p restrained HG-triggered apoptosis of podocytes and inflammatory responses and repressed oxidative stress damage[43]. The miR-15b-5p mimic repressed the viability and inflammation of HG-treated HMCs, as previously shown [42]. The findings show that silencing XIST inhibits HG-induced RTEC pyroptosis *in vitro* by promoting miR-15b-5p. As yet, there have been no studies on the correlation between miR-15b-5p and RTEC pyroptosis in DN, indicating the novelty of our findings.

To study the downstream mechanism of miR-15b-5p, the StarBase website was used to predict that miR-15b-5p can bind to TLR4, which was validated by a dual-luciferase assay and RIP assay. qRT-PCR and Western blotting showed that TLR4 in the DN models was significantly enhanced but was lower

after silencing XIST. The miR-15b-5p inhibitor mitigated the inhibition of TLR4 when XIST was silenced. In summary, XIST inhibits TLR4 by binding to miR-15b-5p. RTEC pyroptosis-induced tubular injury is accompanied by upregulated TLR4 and GSDMD in DN patients[44]. To further verify that the regulation of RTEC pyroptosis by XIST is realized through TLR4, we silenced XIST and overexpressed TLR4 in HG-treated HK2 cells. As expected, TLR4 overexpression promoted IL-1 β , IL-18, NLRP3, ASC, cleaved caspase-1, caspase-1, GSDMD, and GSDMD-N; decreased cell viability; and increased the release rate of LDH. The results of several studies support our findings. TLR4 promotes apoptosis by activating NLRP3/caspase-1[32]. TLR4 depletion inhibits microglial pyroptosis to promote motor function recovery after spinal cord injury[45]. The TLR4 inhibitor TAK-242 induced GSDMD-mediated pyroptosis in HG-exposed cells[44]. In summary, silencing XIST inhibits HG-induced RTEC pyroptosis by inhibiting TLR4.

CONCLUSION

Overall, our results indicate that silencing XIST ultimately relieves renal injury in DN by inhibiting NLRP3/caspase-1-mediated RTEC pyroptosis *via* the ceRNA network of eXIST/miR-15b-5p/TLR4. However, the mechanism of abnormal XIST and miR-15b-5p expression in renal injury in DN has not been comprehensively studied and will be further explored in our future studies. There are many pyroptosis regulatory mechanisms, among which the classical caspase-1 inflammatory body pathway is the most studied. This pathway includes NLRP1, NLRP3, and other nod-like receptor family inflammatory bodies. Here, we investigated the classical caspase-1 pathway. Many studies have shown that the caspase-11 pathway plays an important role in inflammation-related diseases[14,46,47]. We will further explore whether XIST has a regulatory effect on the caspase-11 pathway in future research.

ARTICLE HIGHLIGHTS

Research background

Diabetes is a metabolic disease characterized by hyperglycemia. Chronic hyperglycemia can lead to chronic damage and dysfunction of various tissues and organs, such as eyes, kidneys, heart, blood vessels, and nerves. Various complications caused by diabetes are unavoidable problems in the treatment of diabetes mellitus, including diabetic nephropathy (DN). Understanding the molecular regulation mechanism of DN during renal injury is helpful to the treatment of DN.

Research motivation

Cell pyroptosis is a programmed cell death pattern and plays a key role in DN. However, the regulation mechanism of cell pyroptosis in DN has not been studied clearly. Therefore, our research will help to reveal the role of cell pyroptosis in DN.

Research objectives

Long noncoding RNA X inactive specific transcript (LncRNA XIST) was taken as the main object of our research to explore the molecular mechanism of XIST in pyroptosis of renal tubular epithelial cells (RTECs). We found that XIST comparatively bound to microRNA (miR)-15b-5p to regulate Toll like receptor 4 (TLR4) expression and promote RTEC pyroptosis to participate in kidney injury in DN. Our research results provide a new theoretical basis for the treatment of DN.

Research methods

To study the mechanism of XIST in the pathogenesis of DN-induced pyroptosis, we established DN rat models and high glucose (HG)-induced cell models. By detecting and intervening in the expression of XIST in animal models and cell models, we observed the pathological and representational changes of the models, and collected and analyzed the experimental data. Our research methods conform to science and are carried out strict experimental operation according to the experimental principle, and the results are representative.

Research results

Through experiments, we found that LncRNA XIST was highly expressed in the DN models, and XIST increased the expression of TLR4 as a competing endogenous RNA by competing with miR-15-5p. Inhibiting the expression of XIST repressed the expression of TLR4 by upregulating miR-15-5p, and effectively improved the pyroptosis of RTECs induced by DN. Our findings explain the regulatory mechanism of LncRNA XIST in the pathogenesis of DN-induced RTEC pyroptosis. However, our results have not yet been clinically validated and further exploration is warranted in clinical transformation.

Research conclusions

This study for the first time revealed that lncRNA XIST can enhance the expression of TLR4 through competitively binding to miR-15-5p and promote the pyroptosis of RTECs induced by DN. No new methods were used during the study.

Research perspectives

In the future, we will explore more mechanisms for other targeted miRNAs in the downstream of lncRNA XIST, and we will also study the clinical transformation of XIST/miR-15-5p/TLR4 in DN.

FOOTNOTES

Author contributions: Xu J, Wang Q, and Ren YP designed the research study; Song YF, Xu XH, Zhu H and Chen PD performed the research; Wang Q, Liang L and Xu XH analyzed the data and wrote the manuscript; all authors have read and approve the final manuscript.

Supported by Natural Science Foundation of Shenzhen University General Hospital (SUGH2020QD011).

Institutional animal care and use committee statement: All experiments and procedures were conducted following the laboratory animal care and use guidelines.

Conflict-of-interest statement: For this activity, the authors have no conflicts to declare.

Data sharing statement: No additional data are available.

ARRIVE guidelines statement: The authors have read the ARRIVE guidelines, and the manuscript was prepared and revised according to the ARRIVE guidelines.

Open-Access: This article is an open-access article that was selected by an in-house editor and fully peer-reviewed by external reviewers. It is distributed in accordance with the Creative Commons Attribution NonCommercial (CC BY-NC 4.0) license, which permits others to distribute, remix, adapt, build upon this work non-commercially, and license their derivative works on different terms, provided the original work is properly cited and the use is non-commercial. See: <https://creativecommons.org/licenses/by-nc/4.0/>

Country/Territory of origin: China

ORCID number: Jia Xu 0000-0004-2463-5123; Qin Wang 0000-0002-6135-4135; Yi-Fan Song 0000-0003-4163-4135; Xiao-Hui Xu 0000-0002-4153-2416; He Zhu 0000-0004-2413-6223; Pei-Dan Chen 0000-0003-4136-5136; Ye-Ping Ren 0000-0002-4740-2803.

S-Editor: Wu YXJ

L-Editor: A

P-Editor: Wu RR

REFERENCES

- 1 **Eftekhari A**, Vahed SZ, Kavetsky T, Rameshrad M, Jafari S, Chodari L, Hosseiniyan SM, Derakhshankhah H, Ahmadian E, Ardalan M. Cell junction proteins: Crossing the glomerular filtration barrier in diabetic nephropathy. *Int J Biol Macromol* 2020; **148**: 475-482 [PMID: 31962072 DOI: 10.1016/j.ijbiomac.2020.01.168]
- 2 **Khan NU**, Lin J, Liu X, Li H, Lu W, Zhong Z, Zhang H, Waqas M, Shen L. Insights into predicting diabetic nephropathy using urinary biomarkers. *Biochim Biophys Acta Proteins Proteom* 2020; **1868**: 140475 [PMID: 32574766 DOI: 10.1016/j.bbapap.2020.140475]
- 3 **Dong C**, Liu S, Cui Y, Guo Q. 12-Lipoxygenase as a key pharmacological target in the pathogenesis of diabetic nephropathy. *Eur J Pharmacol* 2020; **879**: 173122 [PMID: 32333927 DOI: 10.1016/j.ejphar.2020.173122]
- 4 **Eisenreich A**, Leppert U. Update on the Protective Renal Effects of Metformin in Diabetic Nephropathy. *Curr Med Chem* 2017; **24**: 3397-3412 [PMID: 28393693 DOI: 10.2174/0929867324666170404143102]
- 5 **Ni WJ**, Ding HH, Tang LQ. Berberine as a promising anti-diabetic nephropathy drug: An analysis of its effects and mechanisms. *Eur J Pharmacol* 2015; **760**: 103-112 [PMID: 25912800 DOI: 10.1016/j.ejphar.2015.04.017]
- 6 **Papadopoulou-Marketou N**, Chrousos GP, Kanaka-Gantenbein C. Diabetic nephropathy in type 1 diabetes: a review of early natural history, pathogenesis, and diagnosis. *Diabetes Metab Res Rev* 2017; **33** [PMID: 27457509 DOI: 10.1002/dmrr.2841]
- 7 **Tesch GH**. Diabetic nephropathy - is this an immune disorder? *Clin Sci (Lond)* 2017; **131**: 2183-2199 [PMID: 28760771 DOI: 10.1042/CS20160636]
- 8 **Yu ZW**, Zhang J, Li X, Wang Y, Fu YH, Gao XY. A new research hot spot: The role of NLRP3 inflammasome activation, a key step in pyroptosis, in diabetes and diabetic complications. *Life Sci* 2020; **240**: 117138 [PMID: 31809715 DOI: 10.1016/j.lfs.2020.117138]

- 10.1016/j.lfs.2019.117138]
- 9 **Xia X**, Wang X, Zheng Y, Jiang J, Hu J. What role does pyroptosis play in microbial infection? *J Cell Physiol* 2019; **234**: 7885-7892 [PMID: 30537070 DOI: 10.1002/jcp.27909]
 - 10 **Zeng C**, Wang R, Tan H. Role of Pyroptosis in Cardiovascular Diseases and its Therapeutic Implications. *Int J Biol Sci* 2019; **15**: 1345-1357 [PMID: 31337966 DOI: 10.7150/ijbs.33568]
 - 11 **Ruan J**, Wang S, Wang J. Mechanism and regulation of pyroptosis-mediated in cancer cell death. *Chem Biol Interact* 2020; **323**: 109052 [PMID: 32169591 DOI: 10.1016/j.cbi.2020.109052]
 - 12 **Ye Z**, Zhang L, Li R, Dong W, Liu S, Li Z, Liang H, Wang L, Shi W, Malik AB, Cheng KT, Liang X. Caspase-11 Mediates Pyroptosis of Tubular Epithelial Cells and Septic Acute Kidney Injury. *Kidney Blood Press Res* 2019; **44**: 465-478 [PMID: 31230050 DOI: 10.1159/000499685]
 - 13 **Lin J**, Cheng A, Cheng K, Deng Q, Zhang S, Lan Z, Wang W, Chen J. New Insights into the Mechanisms of Pyroptosis and Implications for Diabetic Kidney Disease. *Int J Mol Sci* 2020; **21** [PMID: 32992874 DOI: 10.3390/ijms21197057]
 - 14 **Cheng Q**, Pan J, Zhou ZL, Yin F, Xie HY, Chen PP, Li JY, Zheng PQ, Zhou L, Zhang W, Liu J, Lu LM. Caspase-11/4 and gasdermin D-mediated pyroptosis contributes to podocyte injury in mouse diabetic nephropathy. *Acta Pharmacol Sin* 2021; **42**: 954-963 [PMID: 32968210 DOI: 10.1038/s41401-020-00525-z]
 - 15 **Zhan JF**, Huang HW, Huang C, Hu LL, Xu WW. Long Non-Coding RNA NEAT1 Regulates Pyroptosis in Diabetic Nephropathy via Mediating the miR-34c/NLRP3 Axis. *Kidney Blood Press Res* 2020; **45**: 589-602 [PMID: 32721950 DOI: 10.1159/000508372]
 - 16 **Han J**, Zuo Z, Shi X, Zhang Y, Peng Z, Xing Y, Pang X. Hirudin ameliorates diabetic nephropathy by inhibiting Gsdmd-mediated pyroptosis. *Cell Biol Toxicol* 2021 [PMID: 34212273 DOI: 10.1007/s10565-021-09622-z]
 - 17 **Liu P**, Zhang Z, Li Y. Relevance of the Pyroptosis-Related Inflammasome Pathway in the Pathogenesis of Diabetic Kidney Disease. *Front Immunol* 2021; **12**: 603416 [PMID: 33692782 DOI: 10.3389/fimmu.2021.603416]
 - 18 **Lv J**, Wu Y, Mai Y, Bu S. Noncoding RNAs in Diabetic Nephropathy: Pathogenesis, Biomarkers, and Therapy. *J Diabetes Res* 2020; **2020**: 3960857 [PMID: 32656264 DOI: 10.1155/2020/3960857]
 - 19 **Lu J**, Huang Y, Zhang X, Xu Y, Nie S. Noncoding RNAs involved in DNA methylation and histone methylation, and acetylation in diabetic vascular complications. *Pharmacol Res* 2021; **170**: 105520 [PMID: 33639232 DOI: 10.1016/j.phrs.2021.105520]
 - 20 **Li Y**, Xu K, Chen S, Cao Y, Zhan H. Roles of Identified Long Noncoding RNA in Diabetic Nephropathy. *J Diabetes Res* 2019; **2019**: 5383010 [PMID: 30891461 DOI: 10.1155/2019/5383010]
 - 21 **Wang Q**. XIST silencing alleviated inflammation and mesangial cells proliferation in diabetic nephropathy by sponging miR-485. *Arch Physiol Biochem* 2020; 1-7 [PMID: 32669002 DOI: 10.1080/13813455.2020.1789880]
 - 22 **Yang J**, Shen Y, Yang X, Long Y, Chen S, Lin X, Dong R, Yuan J. Silencing of long noncoding RNA XIST protects against renal interstitial fibrosis in diabetic nephropathy via microRNA-93-5p-mediated inhibition of CDKN1A. *Am J Physiol Renal Physiol* 2019; **317**: F1350-F1358 [PMID: 31545928 DOI: 10.1152/ajprenal.00254.2019]
 - 23 **Liu J**, Yao L, Zhang M, Jiang J, Yang M, Wang Y. Downregulation of LncRNA-XIST inhibited development of non-small cell lung cancer by activating miR-335/SOD2/ROS signal pathway mediated pyroptotic cell death. *Aging (Albany NY)* 2019; **11**: 7830-7846 [PMID: 31553952 DOI: 10.18632/aging.102291]
 - 24 **Mafi A**, Aghadavod E, Mirhosseini N, Mobini M, Asemi Z. The effects of expression of different microRNAs on insulin secretion and diabetic nephropathy progression. *J Cell Physiol* 2018; **234**: 42-50 [PMID: 30078212 DOI: 10.1002/jcp.26895]
 - 25 **Xu G**, Mo L, Wu C, Shen X, Dong H, Yu L, Pan P, Pan K. The miR-15a-5p-XIST-CUL3 regulatory axis is important for sepsis-induced acute kidney injury. *Ren Fail* 2019; **41**: 955-966 [PMID: 31658856 DOI: 10.1080/0886022X.2019.1669460]
 - 26 **Li C**, Yang CW, Park CW, Ahn HJ, Kim WY, Yoon KH, Suh SH, Lim SW, Cha JH, Kim YS, Kim J, Chang YS, Bang BK. Long-term treatment with ramipril attenuates renal osteopontin expression in diabetic rats. *Kidney Int* 2003; **63**: 454-463 [PMID: 12631111 DOI: 10.1046/j.1523-1755.2003.00751.x]
 - 27 **Zhang Y**, Tao C, Xuan C, Jiang J, Cao W. Transcriptomic Analysis Reveals the Protection of Astragaloside IV against Diabetic Nephropathy by Modulating Inflammation. *Oxid Med Cell Longev* 2020; **2020**: 9542165 [PMID: 32855769 DOI: 10.1155/2020/9542165]
 - 28 **Liu C**, Zhuo H, Ye MY, Huang GX, Fan M, Huang XZ. LncRNA MALAT1 promoted high glucose-induced pyroptosis of renal tubular epithelial cell by sponging miR-30c targeting for NLRP3. *Kaohsiung J Med Sci* 2020; **36**: 682-691 [PMID: 32391974 DOI: 10.1002/kjm2.12226]
 - 29 **Liu DW**, Zhang JH, Liu FX, Wang XT, Pan SK, Jiang DK, Zhao ZH, Liu ZS. Silencing of long noncoding RNA PVT1 inhibits podocyte damage and apoptosis in diabetic nephropathy by upregulating FOXA1. *Exp Mol Med* 2019; **51**: 1-15 [PMID: 31371698 DOI: 10.1038/s12276-019-0259-6]
 - 30 **Chen X**, Chen RX, Wei WS, Li YH, Feng ZH, Tan L, Chen JW, Yuan GJ, Chen SL, Guo SJ, Xiao KH, Liu ZW, Luo JH, Zhou FJ, Xie D. PRMT5 Circular RNA Promotes Metastasis of Urothelial Carcinoma of the Bladder through Sponging miR-30c to Induce Epithelial-Mesenchymal Transition. *Clin Cancer Res* 2018; **24**: 6319-6330 [PMID: 30305293 DOI: 10.1158/1078-0432.CCR-18-1270]
 - 31 **Tang B**, Li W, Ji T, Li X, Qu X, Feng L, Zhu Y, Qi Y, Zhu C, Bai S. Downregulation of XIST ameliorates acute kidney injury by sponging miR-142-5p and targeting PDCD4. *J Cell Physiol* 2020; **235**: 8852-8863 [PMID: 32347551 DOI: 10.1002/jcp.29729]
 - 32 **El-Sisi AEE**, Sokar SS, Shebl AM, Mohamed DZ, Abu-Risha SE. Octreotide and melatonin alleviate inflammasome-induced pyroptosis through inhibition of TLR4-NF-κB-NLRP3 pathway in hepatic ischemia/reperfusion injury. *Toxicol Appl Pharmacol* 2021; **410**: 115340 [PMID: 33264646 DOI: 10.1016/j.taap.2020.115340]
 - 33 **Umanath K**, Lewis JB. Update on Diabetic Nephropathy: Core Curriculum 2018. *Am J Kidney Dis* 2018; **71**: 884-895 [PMID: 29398179 DOI: 10.1053/j.ajkd.2017.10.026]
 - 34 **Ke R**, Wang Y, Hong S, Xiao L. Endoplasmic reticulum stress related factor IRE1α regulates TXNIP/NLRP3-mediated pyroptosis in diabetic nephropathy. *Exp Cell Res* 2020; **396**: 112293 [PMID: 32950473 DOI: 10.1016/j.yexcr.2020.112293]

- 35 **Lee JY**, Yang JW, Han BG, Choi SO, Kim JS. Adiponectin for the treatment of diabetic nephropathy. *Korean J Intern Med* 2019; **34**: 480-491 [PMID: 31048658 DOI: 10.3904/kjim.2019.109]
- 36 **Miao N**, Yin F, Xie H, Wang Y, Xu Y, Shen Y, Xu D, Yin J, Wang B, Zhou Z, Cheng Q, Chen P, Xue H, Zhou L, Liu J, Wang X, Zhang W, Lu L. The cleavage of gasdermin D by caspase-11 promotes tubular epithelial cell pyroptosis and urinary IL-18 excretion in acute kidney injury. *Kidney Int* 2019; **96**: 1105-1120 [PMID: 31405732 DOI: 10.1016/j.kint.2019.04.035]
- 37 **Yaribeygi H**, Atkin SL, Sahebkar A. Interleukin-18 and diabetic nephropathy: A review. *J Cell Physiol* 2019; **234**: 5674-5682 [PMID: 30417374 DOI: 10.1002/jcp.27427]
- 38 **Fang Y**, Tian S, Pan Y, Li W, Wang Q, Tang Y, Yu T, Wu X, Shi Y, Ma P, Shu Y. Pyroptosis: A new frontier in cancer. *Biomed Pharmacother* 2020; **121**: 109595 [PMID: 31710896 DOI: 10.1016/j.biopha.2019.109595]
- 39 **Qiu Z**, Lei S, Zhao B, Wu Y, Su W, Liu M, Meng Q, Zhou B, Leng Y, Xia ZY. NLRP3 Inflammasome Activation-Mediated Pyroptosis Aggravates Myocardial Ischemia/Reperfusion Injury in Diabetic Rats. *Oxid Med Cell Longev* 2017; **2017**: 9743280 [PMID: 29062465 DOI: 10.1155/2017/9743280]
- 40 **Chang H**, Chang H, Cheng T, Lee GD, Chen X, Qi K. Micro-ribonucleic acid-23a-3p prevents the onset of type 2 diabetes mellitus by suppressing the activation of nucleotide-binding oligomerization-like receptor family pyrin domain containing 3 inflammatory bodies-caused pyroptosis through negatively regulating NIMA-related kinase 7. *J Diabetes Investig* 2021; **12**: 334-345 [PMID: 32881354 DOI: 10.1111/jdi.13396]
- 41 **Chi K**, Geng X, Liu C, Cai G, Hong Q. Research Progress on the Role of Inflammasomes in Kidney Disease. *Mediators Inflamm* 2020; **2020**: 8032797 [PMID: 32410864 DOI: 10.1155/2020/8032797]
- 42 **Chang J**, Yu Y, Fang Z, He H, Wang D, Teng J, Yang L. Long non-coding RNA CDKN2B-AS1 regulates high glucose-induced human mesangial cell injury via regulating the miR-15b-5p/WNT2B axis. *Diabetol Metab Syndr* 2020; **12**: 109 [PMID: 33298110 DOI: 10.1186/s13098-020-00618-z]
- 43 **Fu Y**, Wang C, Zhang D, Chu X, Zhang Y, Li J. miR-15b-5p ameliorated high glucose-induced podocyte injury through repressing apoptosis, oxidative stress, and inflammatory responses by targeting Sema3A. *J Cell Physiol* 2019; **234**: 20869-20878 [PMID: 31025335 DOI: 10.1002/jcp.28691]
- 44 **Wang Y**, Zhu X, Yuan S, Wen S, Liu X, Wang C, Qu Z, Li J, Liu H, Sun L, Liu F. TLR4/NF- κ B Signaling Induces GSDMD-Related Pyroptosis in Tubular Cells in Diabetic Kidney Disease. *Front Endocrinol (Lausanne)* 2019; **10**: 603 [PMID: 31608008 DOI: 10.3389/fendo.2019.00603]
- 45 **Xu S**, Wang J, Jiang J, Song J, Zhu W, Zhang F, Shao M, Xu H, Ma X, Lyu F. TLR4 promotes microglial pyroptosis via lncRNA-F630028O10Rik by activating PI3K/AKT pathway after spinal cord injury. *Cell Death Dis* 2020; **11**: 693 [PMID: 32826878 DOI: 10.1038/s41419-020-02824-z]
- 46 **Wu J**, Sun J, Meng X. Pyroptosis by caspase-11 inflammasome-Gasdermin D pathway in autoimmune diseases. *Pharmacol Res* 2021; **165**: 105408 [PMID: 33412278 DOI: 10.1016/j.phrs.2020.105408]
- 47 **Zhu Y**, Zhao H, Lu J, Lin K, Ni J, Wu G, Tang H. Caspase-11-Mediated Hepatocytic Pyroptosis Promotes the Progression of Nonalcoholic Steatohepatitis. *Cell Mol Gastroenterol Hepatol* 2021; **12**: 653-664 [PMID: 33894425 DOI: 10.1016/j.jcmgh.2021.04.009]



Published by **Baishideng Publishing Group Inc**
7041 Koll Center Parkway, Suite 160, Pleasanton, CA 94566, USA
Telephone: +1-925-3991568
E-mail: bpgoffice@wjgnet.com
Help Desk: <https://www.f6publishing.com/helpdesk>
<https://www.wjgnet.com>

